

RESEARCH ARTICLE

# The Ingenious Structure of Central Rotor Apparatus in $V_oV_1$ ; Key for Both Complex Disassembly and Energy Coupling between $V_1$ and $V_o$

Atsuko Nakanishi<sup>1</sup>\*, Jun-ichi Kishikawa<sup>1</sup>\*, Masatada Tamakoshi<sup>2</sup>, Ken Yokoyama<sup>1</sup>\*

**1** Department of Molecular Biosciences, Kyoto Sangyo University, Motoyama Kamigamo, Kita-ku, Kyoto, Japan, **2** Department of Molecular Biology, Tokyo University of Pharmacy and Life Science, Horinouchi, Hachioji, Tokyo, Japan

\* These authors contributed equally to this work.

\* [yokoken@cc.kyoto-su.ac.jp](mailto:yokoken@cc.kyoto-su.ac.jp)



OPEN ACCESS

**Citation:** Nakanishi A, Kishikawa J-i, Tamakoshi M, Yokoyama K (2015) The Ingenious Structure of Central Rotor Apparatus in  $V_oV_1$ ; Key for Both Complex Disassembly and Energy Coupling between  $V_1$  and  $V_o$ . PLoS ONE 10(3): e0119602. doi:10.1371/journal.pone.0119602

**Academic Editor:** Hendrik W. van Veen, University of Cambridge, UNITED KINGDOM

**Received:** September 9, 2014

**Accepted:** January 14, 2015

**Published:** March 10, 2015

**Copyright:** © 2015 Nakanishi et al. This is an open access article distributed under the terms of the [Creative Commons Attribution License](https://creativecommons.org/licenses/by/4.0/), which permits unrestricted use, distribution, and reproduction in any medium, provided the original author and source are credited.

**Data Availability Statement:** All relevant data are within the paper and its Supporting Information files.

**Funding:** This work was supported by Grants-in-Aid from the Ministry of Education, Science, Sports and Culture of Japan No. 24370059 and 26650039 to KY. The funders had no role in study design, data collection and analysis, decision to publish, or preparation of the manuscript.

**Competing Interests:** The authors have declared that no competing interests exist.

## Abstract

Vacuolar type rotary  $H^+$ -ATPases ( $V_oV_1$ ) couple ATP synthesis/hydrolysis by  $V_1$  with proton translocation by  $V_o$  via rotation of a central rotor apparatus composed of the  $V_1$ -DF rotor shaft, a socket-like  $V_o$ -C (eukaryotic  $V_o$ -d) and the hydrophobic rotor ring. Reconstitution experiments using subcomplexes revealed a weak binding affinity of  $V_1$ -DF to  $V_o$ -C despite the fact that torque needs to be transmitted between  $V_1$ -DF and  $V_o$ -C for the tight energy coupling between  $V_1$  and  $V_o$ . Mutation of a short helix at the tip of  $V_1$ -DF caused intramolecular uncoupling of  $V_oV_1$ , suggesting that proper fitting of the short helix of  $V_1$ -D into the socket of  $V_o$ -C is required for tight energy coupling between  $V_1$  and  $V_o$ . To account for the apparently contradictory properties of the interaction between  $V_1$ -DF and  $V_o$ -C (weak binding affinity but strict requirement for torque transmission), we propose a model in which the relationship between  $V_1$ -DF and  $V_o$ -C corresponds to that between a slotted screwdriver and a head of slotted screw. This model is consistent with our previous result in which the central rotor apparatus is not the major factor for the association of  $V_1$  with  $V_o$  (Kishikawa and Yokoyama, J Biol Chem. 2012 24597-24603).

## Introduction

The Vacuole-type ATPases ( $V_oV_1$ ) are found in many organisms and are involved in a variety of physiological processes [1–3].  $V$ -ATPases in eukaryotic cells (eukaryotic  $V_oV_1$ ) translocate protons across the membrane consuming ATP. Most prokaryotic  $V_oV_1$  (also referred to as  $A$ -ATPase or  $A_oA_1$  [1, 4]) produce ATP using the energy stored in a transmembrane electrochemical proton gradient [3, 5], while the  $V_oV_1$  of some anaerobic bacteria, such as *Enterococcus hirae*, function as a sodium pump [6].

The  $V_oV_1$  and  $F_oF_1$  ATPases/synthases are evolutionarily related and share a rotary mechanism to perform their specific functions [3, 7–9]. The basic structures of the ATPases/synthases are conserved among species [1–3]. The soluble, cytoplasmic portion of  $F_oF_1$  and  $V_oV_1$  (called  $F_1$  and  $V_1$ , respectively), responsible for ATP hydrolysis/synthesis, is connected via the central rotor stalk and the peripheral stator stalk to the transmembrane portion ( $F_o$  and  $V_o$ ) that houses the ion transporting pathway [1–3]. In *Thermus thermophilus*  $V_oV_1$ , the  $V_1$  portion is composed of a hexameric  $A_3B_3$  cylinder and a central shaft comprised of the D and F subunits [3, 10, 11]. The  $V_o$  portion is composed of 5 different subunits with a stoichiometry of  $C_1E_2G_2I_1L_{12}$  (see Fig. 1A). In  $F_oF_1$ , a  $\gamma$ -subunit (equivalent to subunits D and F of  $V_oV_1$ ) binds directly to the rotor ring [12]. In contrast, at the boundary surface of  $V_oV_1$ ,  $V_o$ -C forms a socket-like structure which accommodates the  $V_1$ -DF central shaft [13], indicating that  $V_1$ -DF does not contact the rotor ring directly. Thus, the boundary surface of  $V_oV_1$  is significantly different from that in  $F_oF_1$ .  $V_oV_1$  also has a more complex peripheral stalk structure than  $F_oF_1$ . The stator structure of  $F_oF_1$  consists of a single peripheral stalk, while  $V_1$  is connected with  $V_o$  by two or three peripheral stalks [4, 14, 15].

Recent reconstitution studies of *T. thermophilus*  $V_oV_1$  have demonstrated that the  $A_3B_3$  domain is tightly associated with the two EG peripheral stalks of  $V_o$ , even in the absence of the central shaft subunits [16]. In other words, the peripheral stalks are the major factor mediating association of  $V_1$  and  $V_o$ , consistent with the unique boundary surface between  $V_1$ -DF and  $V_o$ -C in  $V_oV_1$ . This arrangement is highly relevant for the detachment of  $V_1$ -DF from  $V_o$ -C [13, 16]. However torque needs to be transmitted between  $V_1$ -DF and  $V_o$ -C for tight energy coupling between  $V_1$  and  $V_o$  [16]. Thus a sticky interaction which also allows detachment of  $V_1$ -DF from  $V_o$ -C is required. How the protein maintains these two somewhat contradictory properties has yet to be investigated.

Lau *et al.* reported a sub-nanometer resolution structure of *T. thermophilus*  $V_oV_1$  by single particle cryo-electron microscopy [11] showing that the rod like structure of  $V_1$ -DF is positioned in the cavity of  $V_o$ -C. This suggests that the rod like structure might play an important role in binding of  $V_1$ -DF and  $V_o$ -C. A crystal structure of  $V_1$ -DF isolated from *E. hirae*  $V_oV_1$  suggested that the rod like structure might be a short helix at the tip of the  $V_1$ -DF (Fig. 1B, [17]).

In this study, reconstitution and fluorescence resonance energy transfer (FRET) analysis of  $V_oV_1$  subcomplexes reveal that the binding affinity of  $V_1$ -DF with  $V_o$ -C subunit is weak. Further investigations indicated that the short helix of the  $V_1$ -DF subunit has important roles in both reconstitution of  $V_oV_1$  and torque transmission. We propose a structural model accounting for both the detachable and sticky nature of the interaction between  $V_1$ -DF and  $V_o$ -C.

## Materials and Methods

### Proteins isolation of $V_o$ and $CL_{12}$

Wild-type or mutant  $V_oV_1$  (C-T105C/C-C268S/C-C323S) from *T. thermophilus* strains incorporating a His<sub>3</sub> tag on the C terminus of subunit L were generated by the integration vector system [18]. Culture of the modified *T. thermophilus* strains, membrane preparation, solubilization of His-tagged  $V_oV_1$  and purification of  $V_oV_1$ ,  $V_o$  and  $CL_{12}$  were carried out as described previously [19]. The mutated  $V_o$  and  $CL_{12}$  (C-T105C/C-C268S/C-C323S) were used for the FRET experiments.

### Preparation of $V_1$ ( $A_3B_3DF$ ) and $V_1$ -DF

*Escherichia coli* strain BL21-CodonPlus-RP (Stratagene) was used for expression of  $V_1$  ( $A_3B_3DF$ ) and  $V_1$ -DF. These recombinant subcomplexes were isolated as described previously [20, 21]. The expression plasmids for  $V_1$  containing DF from *H. sapiens* or *E. hirae* were constructed by the



swapped short helix of *E. hirae* were constructed by PCR mutagenesis. To introduce the swapped short helix of *E. hirae*, complementary oligonucleotide primers containing the sequences encoding the 8 amino acids of this region were used to amplify the gene fragment. The fragment was then digested with appropriate restriction enzymes, and inserted into the corresponding region of the *T. thermophilus*  $V_1$  expression plasmid [20]. The mutant  $V_1$  (A-His<sub>8</sub>/ΔCys, A-C255A/A-S232A/A-T235S, F-S54C) and mutant DF (F-His<sub>6</sub>, S54C) were used for either reconstitution or FRET experiments [16].

### Reconstitution of $V_0V_1$

The purity of each subcomplex was confirmed by SDS-PAGE.  $V_1$  or  $V_1$ -DF (each 1 mg/ml) in MOPDM buffer (50 mM MOPS (pH 7.0), 150 mM NaCl, 0.03% n-dodecyl-β-D-maltoside) was mixed with 1 mg/ml  $V_0$  or  $CL_{12}$  at an equal volume ratio. The mixtures were incubated for 1 h at 25°C and then applied onto the Superdex HR-200 column equilibrated with the same buffer. The reconstituted  $V_0V_1$  were collected and used for further analysis immediately.

### FRET analysis

FRET analysis was carried out as described previously [16]. The purified  $V_1$  (A-His<sub>8</sub>/ΔCys, A-S232A/A-T235S, F-S54C) or DF (F-His<sub>6</sub>, S54C) was immediately labeled with an excess amount of Cy3-maleimide (GE healthcare, used as a donor molecule) in MOPDM buffer. Following a 60 min incubation at 25°C, proteins were separated from unbound reagent with a PD-10 column (GE Healthcare). The mutated  $V_0$  (C-T105C/C-C268S/C-C323S) was labeled with Cy5-maleimide (GE Healthcare, used as an acceptor molecule) by the same method described above. The specific labeling of subunit F in  $V_1$  or DF, and subunit C in  $V_0$  or  $CL_{12}$  was checked by measurement of subunit fluorescence. FRET, as a result of reconstitution of  $V_0V_1$ , was monitored with a fluorimeter using an excitation wavelength of 532 nm and an emission wavelength of 570 nm (FP-6200, JASCO). A cuvette was filled with 1.2 ml of MOPDM buffer containing 2 nM labeled  $V_1$  or DF and incubated at 25°C until the fluorescence intensity reached a constant level. For measurement of binding kinetics, 8.0 μl of labeled  $V_0$  or  $CL_{12}$  was added into the cuvette at a final concentration of 10 nM.

### Measurements of ATP synthesis of the $V_0V_1$

The reconstituted complexes were incorporated into liposomes using a freeze-thaw method [23]. Acidification of the proteoliposomes and measurement of ATP synthesis were carried out at 25°C. To acidify the interior of proteoliposomes, 30 μl of the proteoliposome solution was mixed with 15 μl of acidification buffer (300 mM MES pH4.7) and then incubated for 5 min at 25°C. The ATP was measured as the increase of intensity of luminescence in a Luminescencer-PSN (ATTO). The ATP synthesis reaction was initiated by injection of 30 μl of the acidified proteoliposomes into 0.5 ml of base buffer containing 100 mM Tricin-sodium (pH 8.5), 2.5 mM MgSO<sub>4</sub>, 10 mM phosphate, 2.2 mg of luciferin/luciferase compound, 0.5 mM ADP, 36 nM valinomycin, and 100 mM KCl. For calibration, ATP was injected into the base buffer.

### Measurements of proton channel and proton pump activity by the $V_0V_1$

Crude soybean L-α-Phosphatidylcholine (Sigma) was washed with 20 mM Tricine-sodium (pH 8.5), 2.5 mM MgSO<sub>4</sub> to remove K<sup>+</sup> as described [24]. K<sup>+</sup>-loaded proteoliposomes containing enzyme were prepared as follows; aliquots containing reconstituted complex were diluted to 0.5 mg/ml in 20 mM Tricine, 2.5 mM MgCl<sub>2</sub> 20 mM MES pH8.0, 4% n-Octyl-β-D-glucoside (Sigma), the washed 20 mg/ml lipid and 150 mM KCl for the measurement of proton pump or

500mM KCl for the measurement of proton channel activity. Bio-beads SM-2 (Bio-Rad) were added to remove the detergent and incubated for 2 h at 25°C. Resultant proteoliposomes were centrifuged and subjected to the proton pump and proton channel analysis.

The acidification of liposomes was measured by the quenching of 9-amino-6-chloro-2-methoxyacridine, (ACMA) (Sigma) fluorescence [25]. Aliquots containing 5  $\mu$ g of protein were suspended in 1.2 ml of 20 mM Tricine, 2.5 mM  $MgCl_2$ , 40 mM MES pH8.0, 500 mM NaCl for the measurement of proton channel or 110 mM NaCl /40 mM KCl for the measurement of proton pump activity, in the presence of 15 ng of ACMA. The time course of fluorescence quenching was monitored using a fluorimeter (FP-6200, JASCO).

## Other assays

Protein concentrations of  $V_1$  were determined from UV absorbance calibrated by quantitative amino acid analysis; 1 mg/ml gives an optical density of 0.88 at 280 nm. Protein concentrations of  $V_o$  and  $V_oV_1$  were determined by BCA protein assay, with BSA used as the protein standard. ATPase activity was measured at 25°C with an enzyme-coupled ATP regenerating system [5]. Polyacrylamide gel electrophoresis in the presence of SDS or AES was carried out as described previously [5]. The proteins were stained with Coomassie Brilliant Blue.

## Results

### Weak interaction at the boundary surface between $V_1$ -DF and $CL_{12}$

Reconstitution of  $A_3B_3$  and  $V_o$  has indicated that the interaction between  $A_3B_3$  and two EG peripheral stalks is rigid [16]. However the precise nature of the interaction between  $V_1$ -DF and  $V_o$ -C has not been experimentally characterized. In order to examine the interaction the isolated  $V_1$ -DF subunits or subcomplexes from  $V_1$  with  $V_o$  or  $CL_{12}$ , were mixed with  $V_o$  or  $CL_{12}$ . The purity and subunit stoichiometry of all subcomplexes were confirmed by both SDS-PAGE and AES-PAGE (Fig. 2A and B). The band corresponding to  $V_1$ -DF was not detected on AES-PAGE gel. Reconstituted  $V_oV_1$  was identified as a single band on AES-PAGE when  $V_1$  was incubated with  $V_o$  at a molar ratio of 1:1 (Fig. 2B, lane 5). However attempts to reconstitute  $V_1$  with  $CL_{12}$  were unsuccessful as assessed by both AES-PAGE and gel permeation analysis (Fig. 2B, lane 6 and Fig. 2C, line 7). The same was also true for  $V_1$ -DF and  $CL_{12}$  or  $V_o$  (Fig. 2B, lane 7 and Fig. 2C, line 6 and 8). Together, these results strongly suggest that the interaction of the boundary surface between  $V_1$ -DF and  $V_o$ -C in the complex is insufficient for reconstitution of a stable complex.

Further analysis of the interaction at the boundary surface between  $V_1$ -DF and  $V_o$ -C was carried out by fluorescent resonance of energy transfer (FRET), a powerful method for detecting protein-protein interaction/association [16]. For FRET analysis, each component was labeled with Cy3 or Cy5 (fluorescent dyes as described in ref. [16]). A mutated  $V_1$ -DF or  $V_1$  incorporating a single cysteine residue (F/S54C) was labeled with Cy3 as a donor, while a mutated  $V_o$  or  $CL_{12}$  (C/T105C) was labeled with Cy5 as an acceptor. Reconstitutions were carried out in a cuvette containing 1.2 ml of the 2 nM  $V_1$  or  $V_1$ -DF labeled with Cy3. The reconstitution efficiency was evaluated by the decrease in donor emission (Fluorescence at 570 nm, ref. [16]). As shown in Fig. 2D, the fluorescence of  $V_1$  decreased sharply upon addition of  $V_o$  into the cuvette, indicating reconstitution of  $V_1$  and  $V_o$  complex (purple line). In contrast, addition of 8.0  $\mu$ l of 1.5 mM of  $CL_{12}$  or  $V_o$  into a cuvette containing  $V_1$ -DF exhibited no decrease in fluorescence at 570 nm (red or blue lines). Furthermore the addition of 8.0  $\mu$ l of 1.5 mM of  $CL_{12}$  into a cuvette containing  $V_1$  showed no decrease in fluorescence (green line). These results clearly indicate low binding affinity between  $V_1$ -DF and  $V_o$ -C, consistent with the findings from the reconstitution experiments [16].

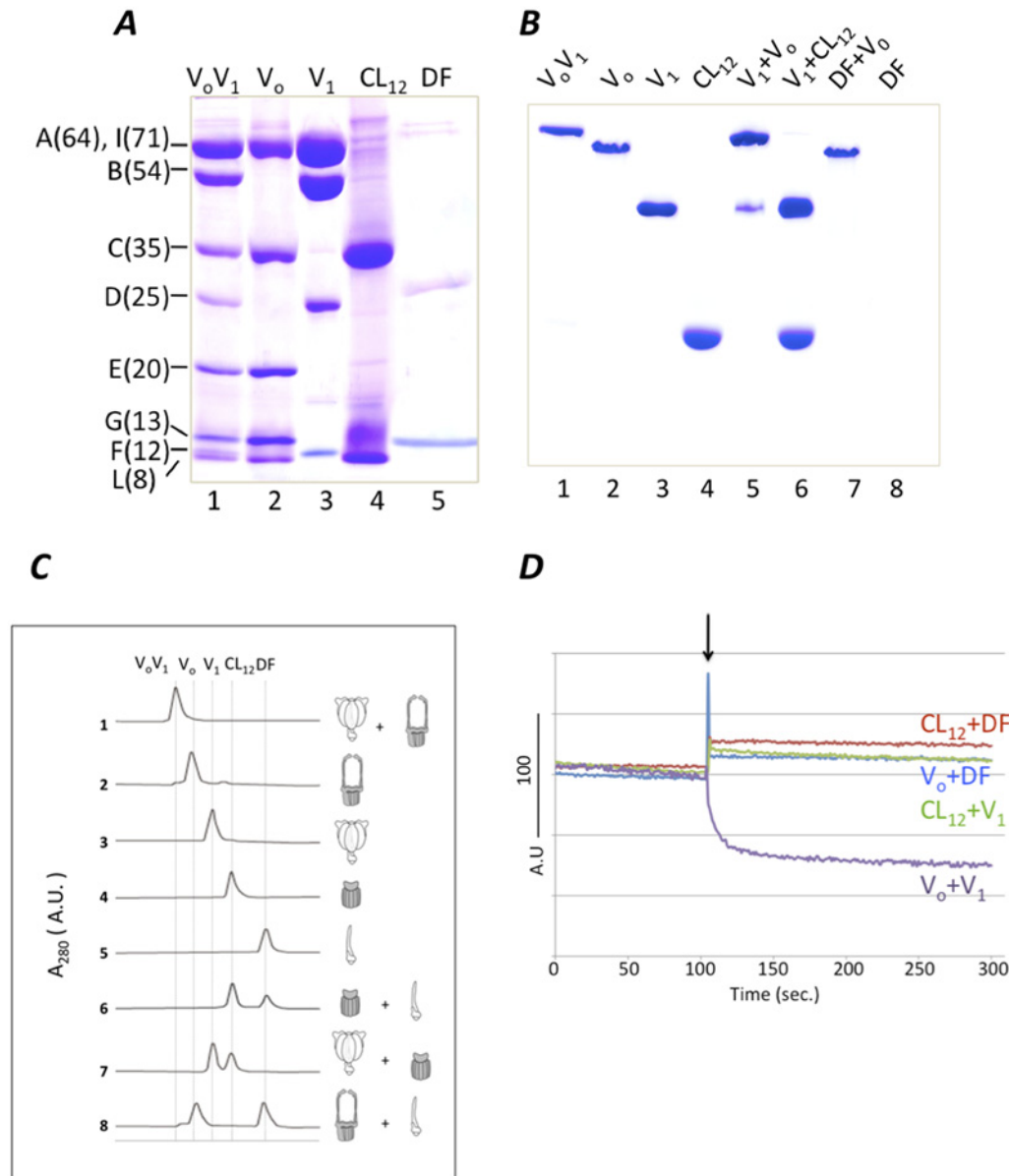


**Fig 2. Analysis of reconstitution of complexes and subcomplexes.** A, 15% SDS-PAGE analysis. Lane 1,  $V_0V_1$ ; lane 2,  $V_0$ ; lane 3  $V_1$ ; lane 4,  $CL_{12}$ ; lane 5, DF. Molecular weights of each subunit are indicated in parentheses. B, 6% AES-PAGE. The mixtures containing the subcomplexes were incubated for 1h at 25°C respectively, prior to analysis. Lane 1,  $V_0V_1$ ; lane 2,  $V_0$ ; lane 3,  $V_1$ ; lane 4,  $CL_{12}$ ; lane 5,  $V_0$  and  $V_1$ ; lane 6,  $V_1$  and  $CL_{12}$ ; lane 7, DF and  $V_0$ ; lane 8; DF. The band of DF complex was not detected on AES-PAGE gel. C, Gel permeation analysis of complexes and subcomplexes. The mixtures containing subcomplexes indicated by the scheme were incubated for 1h at 25°C respectively, followed by analysis. The molecular weights of each complex are,  $V_0V_1$  (659kDa),  $V_0$  (268kDa),  $V_1$  (391 kDa),  $CL_{12}$  (131 kDa) and  $V_1$ -DF (37 kDa). D, FRET analysis of reconstituted complexes and subcomplexes. Fluorescence of 3 nM  $V_1$ -Cy3 (purple and green lines) or 3 nM  $V_1$ -DF-Cy3 (blue and red lines) was recorded (excitation at 532nm) before and after addition of  $V_0$ -Cy5 or  $CL_{12}$ -Cy5. The  $V_0$ -Cy5 or  $CL_{12}$ -Cy5 was added at the time indicated by the arrow.

doi:10.1371/journal.pone.0119602.g002

### Effect of exogenous $V_1$ -DF on reconstitution of $V_1$ and $V_0$

The amino acid sequence of  $V_1$ -DF is not highly conserved among species (Fig. 1C). To investigate the effect of these differences on reconstitution of  $V_1$  and  $V_0$ , expression constructs of  $V_1$  containing  $V_1$ -DF from *Homo sapiens* ( $V_1$ -DF-*H.s.*) or *E. hirae* ( $V_1$ -DF-*E.h.*) were generated. These chimeric  $V_1$  were purified and subjected to ATPase analysis as described in Materials and

Methods. Subunit stoichiometry of each chimeric  $V_1$  was confirmed by SDS-PAGE analysis (Fig. 3A). These chimeric  $V_1$  were ATPase active (Table 1, S1 Fig.), indicating that the exogenous  $V_1$ -DF functions as a rotor in  $A_3B_3$  of *T. thermophilus*. As shown in Table 1, the presence of the exogenous DF shaft from *H. sapiens* markedly enhanced the ATPase activity of  $V_1$ . The enhanced ATPase activity of chimeric  $V_1$  is likely due to primary sequence difference between the DF of *T. thermophilus* and that of *H. sapiens*. We will discuss the effect of the *H. sapiens* DF on the activity of  $V_1$  fully elsewhere.

Each chimeric  $V_1$  was mixed with an excess amount of  $V_o$  from *T. thermophilus* and incubated for 1 hour. Analysis by gel permeation analysis revealed peaks corresponding to reconstituted  $V_oV_1$  containing the exogenous  $V_1$ -DF (Fig. 3B, lines 9 and 10). Subunit stoichiometry of the fraction containing each chimeric  $V_oV_1$  was confirmed by SDS-PAGE analysis (Fig. 3C). These results indicate that the chimeric  $V_1$  incorporating the exogenous  $V_1$ -DF can assemble with  $V_o$ .

### Role of the short helix of $V_1$ -D subunit in interaction of $V_1$ and $V_o$

The EM density structure of intact  $V_oV_1$  of *T. thermophilus* and the crystal structure of  $V_1$ -DF suggested that an  $\alpha$ -helix of  $V_1$ -D (a.a. 73–80) is key for interaction between  $V_1$ -DF and  $V_o$ -C ([11,17] and Fig. 1B and C). This helix is referred to as the short helix hereafter. To investigate the role of the short helix in reconstitution of  $V_1$  and  $V_o$ ,  $V_{1-SH-E.h}$  containing the exogenous short helix of *E. hirae* ( $A^{74}$ FIDELLA<sup>81</sup>, Fig. 1C), and  $V_{1\Delta SH}$  lacking the short helix of the  $V_1$ -DF were constructed. The subunit stoichiometry and purity of the mutated  $V_1$  constructs were confirmed by SDS-PAGE analysis (Fig. 3A). Reconstitution of  $V_o$  and  $V_{1-SH-E.h}$  or  $V_{1\Delta SH}$  was confirmed by gel permeation and FRET analysis (Fig. 3B, line 11, 12). Subunit stoichiometry of the fraction containing each mutated  $V_oV_1$  was confirmed by SDS-PAGE analysis (Fig. 3C). These findings indicate that the short helix is not essential for reconstitution of  $V_1$  with  $V_o$ .

### Role of the short helix of $V_1$ -D subunit in energy coupling between $V_1$ and $V_o$

To further investigate the role of the short helix of the  $V_1$ -D subunit in energy coupling between  $V_1$  and  $V_o$ , ATP synthesis activity of the reconstituted  $V_oV_1$  were assessed. The reconstituted  $V_oV_1$  constructs were purified by gel permeation chromatography and reconstituted into liposomes by freeze-thaw methods. Proton motive force was generated across the membranes of the reconstituted liposomes by acid-base transition (ref. [23], see inset in Fig. 4A). As shown in Fig. 4A, wild type reconstituted  $V_oV_1$  showed continuous ATP synthesis. In contrast, the reconstituted  $V_oV_{1\Delta SH}$  showed no ATP synthesis activity, indicating that lack of the short helix in  $V_oV_1$  causes an intra molecular uncoupling between  $V_1$  and  $V_o$ . In addition, the reconstituted  $V_oV_1$  including the exogenous  $V_1$ -DF ( $V_oV_{1-DF-H.s}$ ,  $V_oV_{1-DF-E.h}$ ) or the short helix ( $V_oV_{1-SH-E.h}$ ) showed no ATP synthesis activity.

Next, proton channel and proton pump activity of the reconstituted  $V_oV_1$  were measured to investigate the energy coupling efficiency between the mutated  $V_1$  and  $V_o$  in the complexes. To facilitate ATP hydrolysis activity measurements, a mutated  $V_1$  incorporating the TSSA substitutions (A-S232A/A-T235S) to overcome ADP inhibition was used [5]. The wild-type  $V_oV_1$  did not show proton channel activity but did show proton pump activity (Fig. 4B, C). These results indicate that the wild-type  $V_oV_1$  is tightly coupled. In contrast, mutated  $V_oV_1$  including the exogenous short helix or lacking the short helix did not show proton pump activity (Fig. 4C). In contrast, the mutated  $V_oV_1$ s had proton pump activity almost identical to the proton channel activity of  $V_o$  (Fig. 4B), indicating that the mutated  $V_oV_1$ s were completely



**Table 1. Kinetics parameters of the mutated  $V_1$  for ATPase activity.**

	$V_1$	$V_{1-E.H-DF}$	$V_{1-H.S-DF}$	$V_{1-SH-E.H}$	$V_{1\Delta SH}$
$K_m$ [mM]	$0.23 \pm 0.05$	$0.76 \pm 0.04$	$0.48 \pm 0.04$	$0.22 \pm 0.05$	$0.24 \pm 0.06$
$V_{max}$ [ $s^{-1}$ ]	$30.6 \pm 1.8$	$38.0 \pm 0.80$	$132 \pm 3.0$	$27.5 \pm 1.5$	$21.8 \pm 1.4$

$K_m$  and  $V_{max}$  values represent means  $\pm$  SD ( $n = 3$ ).

doi:10.1371/journal.pone.0119602.t001

uncoupled. These results strongly suggest that a proper match between the short helix in  $V_1$ -D subunit and  $V_o$ -C subunit is essential for tight energy coupling between  $V_1$  and  $V_o$ .

## Discussion

In this study, we have directly demonstrated a low binding affinity between  $V_1$ -DF and  $V_o$ -C by both FRET and reconstitution experiments (Fig. 2). This is consistent with our previous result indicating that the two EG peripheral stalks are the major mediators of association of  $V_1$  with  $V_o$  [16]. This low binding affinity between  $V_1$ -DF and  $V_o$ -C is relevant to reversible dissociation/association of  $V_1$  from  $V_o$  in eukaryotic  $V_oV_1$  [26, 27]. However such low binding affinity is unfavorable for energy coupling between  $V_1$  and  $V_o$ ; for ATP synthesis ( $\Delta G = \sim 55$  kJ/mol, [16]), the torque generated in the  $V_o$  rotor ring needs to be transmitted to  $V_1$ -DF via  $V_o$ -C. Thus, an ingenious structure, that is both detachable and sticky, is required at the boundary surface between  $V_1$ -DF and  $V_o$ -C. The EM density map of *T. thermophilus*  $V_oV_1$  [11] provided a clue to unraveling the molecular basis of these seemingly contradictory properties. The short helix of  $V_1$ -DF apparently lies in the cavity of  $V_o$ -C in  $V_o$ , suggesting that it may play an important role in association of  $V_1$ -DF and  $V_o$ -C.

Here, we have investigated the role of the short helix in  $V_1$ -D subunit on  $V_oV_1$  assembly and energy coupling between  $V_1$  and  $V_o$ . Not only the chimeric  $V_1$  containing the exogenous  $V_1$ -DF and the short helix, but also  $V_1$  lacking the short helix could reconstitute the complex with  $V_o$  (Fig. 3), indicating that the short helix is not a key factor for  $V_oV_1$  complex formation. However, these mutant  $V_oV_1$ s showed neither ATP synthesis or proton pump activities (Fig. 4). As shown in Fig. 1C, amino acid residues in the short helix of  $V_1$ -D are not highly conserved among species (*T. thermophilus*, *E. hirae*, *H. sapiens*). The different surface shape of the exogenous short helix compared to the endogenous one likely generates repulsion between  $V_1$ -DF and  $V_o$ -C. The intact fitting of the short helix into the recess of  $V_o$ -C appears to be required for tight energy coupling between  $V_1$  and  $V_o$ .

Here we propose a model to account for a detachable  $V_1$ -DF/ $V_o$ -C boundary surface, which can transmit torque. In this model, the relationship between  $V_1$ -DF and  $V_o$ -C is analogous to that between a slotted screwdriver and a head of slotted screw (Fig. 5). In the  $V_oV_1$ , two EG peripheral stalks push the short helix of  $V_1$ -D into the socket of  $V_o$ -C. Thus, the short helix of  $V_1$ -D binds into the socket of  $V_o$ -C, forming a sufficiently close interaction for transmission of torque from the rotating  $V_1$ -DF to  $V_o$ -C. The rigid interaction between the  $V_1$ -DF and  $V_o$ -C would be abolished by a loss of interaction between the two EG peripheral stalks and  $A_3B_3$ , consistent with the results of reconstitution experiments (Fig. 2) and EM analysis of sequential disassembly of the  $V_oV_1$  [28].  $F_oF_1$  does not contain a counterpart of  $V_o$ -C so that the  $F_1$  shaft composed of the  $\gamma$  subunit directly attaches to the  $c_{6-10}$  rotor ring [12]. Thus, the  $F_1$ - $c_{6-10}$  stator-less complex is easily isolated from  $F_oF_1$ .

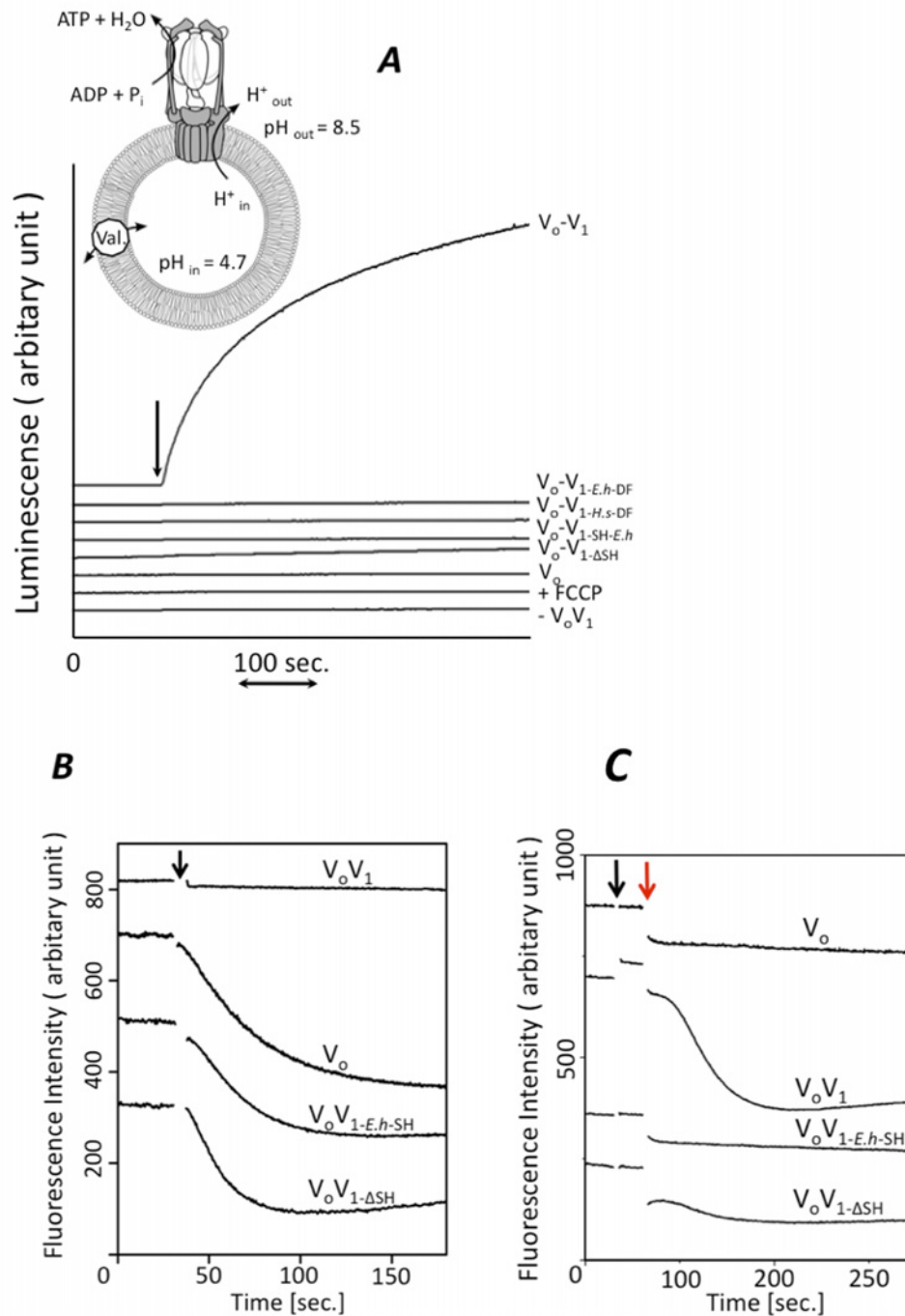


**Fig 4. Function of the short helix of  $V_1$ -D subunit for energy coupling.** A, Analysis of ATP synthesis by the reconstituted complexes. *inset*; schematic model of the experimental system [16]. The reconstituted  $V_0V_1$  was incorporated into liposomes, then energized by an acid base transition procedure described in the Materials and Methods. Each line shows the raw data for ATP synthesis by each reconstituted complex at a  $\Delta$  pH of 3.8. The reactions were initiated by addition of acidified proteoliposomes into the base buffer, as indicated by the arrow. Final concentrations were 2  $\mu$ g/ml of  $V_0V_1$  and 1 mM ADP. The synthesized ATP was monitored by the luciferin-luciferase assay [18]. Analysis of proton channel (B) and proton pump activity (C) coupled with ATP hydrolysis by proteoliposomes.  $K^+$ -loaded proteoliposomes containing the reconstituted complexes were prepared as described in the Materials and Methods. Proton influx was initiated by addition of 20 ng of valinomycin at the time indicated by the black arrow (B) and proton pump was initiated by addition of ATP-Mg at finally 1mM followed by the addition of valinomycin at the time indicated by the red arrow (C). The ACMA fluorescence emission (480nm) was recorded at 25°C.

doi:10.1371/journal.pone.0119602.g004

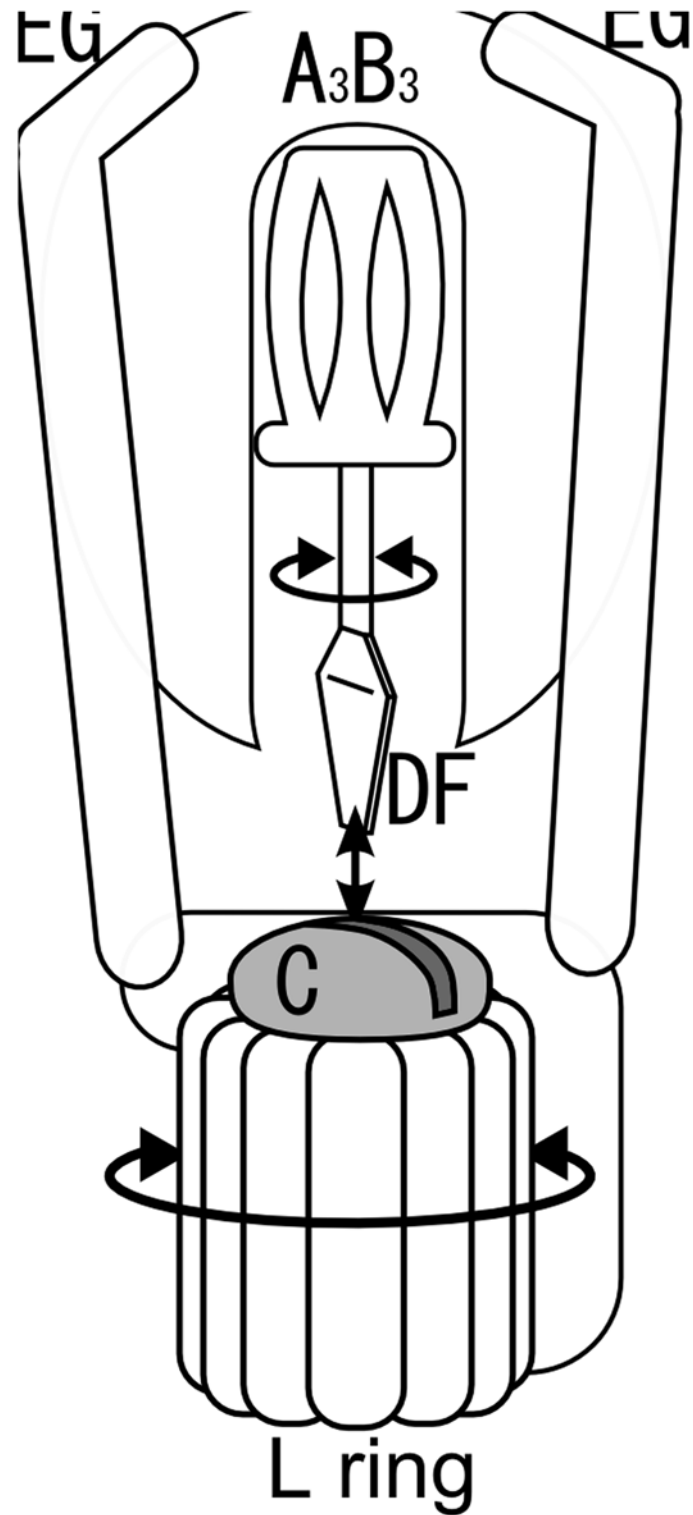


**Fig 5. A schematic diagram for a slotted screwdriver and a head of slotted screw in  $V_0V_1$  [16].**

doi:10.1371/journal.pone.0119602.g005

## Supporting Information

**S1 Fig. [S]-V plot of ATP hydrolysis rate catalyzed by mutated  $V_1$ .** The solid lines show fit with the Michaelis-Menten equation.  
(TIF)

## Acknowledgments

We thank Dr. Bernadette Byrne for critical reading of the manuscript, Dr Takeshi Murata for the gift of pCempt18.

## Author Contributions

Conceived and designed the experiments: KY. Performed the experiments: AN JK MT. Analyzed the data: AN JK. Contributed reagents/materials/analysis tools: MT. Wrote the paper: KY AN JK.

## References

1. Forgac M. Vacuolar ATPases: rotary proton pumps in physiology and pathophysiology. *Nat. Rev. Mol. Cell Biol.* 2007; 8: 917–929 PMID: [17912264](#)
2. Mulkidjanian AY, Makarova KS, Galperin MY, Koonin EV. Inventing the dynamo machine: the evolution of the F-type and V-type ATPases. *Nat. Rev. Microbiol.* 2007; 5: 892–899. PMID: [17938630](#)
3. Yokoyama K, Imamura H. Rotation, structure, and classification of prokaryotic V-ATPase. *J. Bioenerg. Biomembr.* 2005; 37: 405–410 PMID: [16691473](#)
4. Muench SP, Trinick J, Harrison MA. Structural divergence of the rotary ATPase. *Q. Rev. Biophys.* 2011; 44: 311–356 doi: [10.1017/S0033583510000338](#) PMID: [21426606](#)
5. Nakano M, Imamura H, Toei M, Tamakoshi M, Yoshida M, Yokoyama K. ATP hydrolysis and synthesis of a rotary motor V-ATPase from *Thermus thermophilus*. *J. Biol. Chem.* 2008; 283: 20789–20896
6. Kakinuma Y, Yamato I, Murata T. Structure and function of vacuolar  $\text{Na}^+$ -translocating ATPase in *Enterococcus hirae*. *J. Bioenerg. Biomembr.* 1999; 31: 7–14 PMID: [10340844](#)
7. Yoshida M, Muneyuki E, Hisabori T. ATP synthase—a marvellous rotary engine of the cell. *Nat. Rev. Mol. Biol.* 2001; 2: 669–677 PMID: [11533724](#)
8. Kishikawa J, Ibuki T, Nakamura S, Nakanishi A, Minamino T, Miyata T, et al. Common evolutionary origin for the rotor domain ATPase and flagellar protein export apparatus. *PLoS ONE.* 2013; 8: e64695 doi: [10.1371/journal.pone.0064695](#) PMID: [23724081](#)
9. Jefferies KC, Cipriano DJ, Forgac M. Function, structure and regulation of the vacuolar  $\text{H}^+$ -ATPases. *Arch Biochem Biophys.* 2008; 476: 33–42. doi: [10.1016/j.abb.2008.03.025](#) PMID: [18406336](#)
10. Nagamatsu Y, Takeda K, Kuranaga T, Numoto N, Miki K. Origin of asymmetry at the intersubunit interfaces of  $V_1$ -ATPase from *Thermus thermophilus*. *J. Mol. Biol.* 2013; 425: 2699–2708 doi: [10.1016/j.jmb.2013.04.022](#) PMID: [23639357](#)
11. Lau WC, Rubinstein JL. Subnanometre-resolution structure of the intact *Thermus thermophilus*  $\text{H}^+$ -driven ATP synthase. *Nature* 2011; 481: 214–218
12. Stock D, Leslie AG, Walker JE. Molecular architecture of the rotary motor in ATP synthase. *Science* 1999; 286: 1700–1705 PMID: [10576729](#)
13. Iwata M, Imamura H, Stambouli E, Ikeda C, Tamakoshi M, Nagata K, et al. Crystal structure of a central stalk subunit C and reversible association/dissociation of vacuole-type ATPase. *Proc. Natl. Acad. Sci. U.S.A.* 2004; 101: 59–64 PMID: [14684831](#)
14. Stewart AG, Lee LK, Donohoe M, Chaston JJ, Stock D. The dynamic stator stalk of rotary ATPase. *Nature Commun.* 2012; 3:687.
15. Kitagawa N, Mazon H, Heck AJ, Wilkens S. Stoichiometry of the peripheral stalk subunits E and G of yeast  $V_1$ -ATPase determined by mass spectrometry. *J. Biol. Chem.* 2008; 283: 3329–37
16. Kishikawa J, Yokoyama K. Reconstitution of Vacuolar type rotary  $\text{H}^+$ -ATPase/synthase from *Thermus thermophilus*. *J. Biol. Chem.* 2012; 287: 24597–24603 doi: [10.1074/jbc.M112.367813](#) PMID: [22582389](#)

17. Saijo S, Arai S, Hossain KM, Yamato I, Suzuki K, Kakinuma Y, et al. Crystal structure of the central axis DF complex of the prokaryotic V-ATPase. *Proc. Natl. Acad. Sci. U.S.A.* 2011; 108: 19955–19960 doi: [10.1073/pnas.1108810108](https://doi.org/10.1073/pnas.1108810108) PMID: [22114184](https://pubmed.ncbi.nlm.nih.gov/22114184/)
18. Tamakoshi M, Uchida M, Tanabe K, Fukuyama S, Yamagishi A, Oshima T. A new *Thermus-Escherichia coli* shuttle integration vector system. *J. Bacteriol.* 1997; 179: 4811–4814 PMID: [9244269](https://pubmed.ncbi.nlm.nih.gov/9244269/)
19. Yokoyama K, Nagata K, Imamura H, Ohkuma S, Yoshida M, Tamakoshi M. Subunit arrangement in V-ATPase from *Thermus thermophilus*. *J. Biol. Chem.* 2003; 278: 42686–42691 PMID: [12913005](https://pubmed.ncbi.nlm.nih.gov/12913005/)
20. Imamura H, Ikeda C, Yoshida M, Yokoyama K. The F subunit of *Thermus thermophilus*  $V_1$ -ATPase promotes ATPase activity but is not necessary for rotation. *J. Biol. Chem.* 2004; 279: 18085–18090 PMID: [14963028](https://pubmed.ncbi.nlm.nih.gov/14963028/)
21. Kishikawa J, Nakanishi A, Furuie S, Tamakoshi M, Yokoyama K. Molecular basis of ADP inhibition of vacuolar (V)-type ATPase/synthase. *J. Biol. Chem.* 2014; 289: 403–412
22. Murata T, Takase K, Yamato I, Igarashi K, Kakinuma Y. Properties of the  $V_0V_1Na^+$ -translocating ATPase from *Enterococcus hirae* and its  $V_0$  moiety. *J. Biochem.* 1999; 125: 414–421 PMID: [9990142](https://pubmed.ncbi.nlm.nih.gov/9990142/)
23. Toei M, Gerle C, Nakano M, Tani K, Gyobu N, Tamakoshi M, et al. Dodecamer rotor ring defines  $H^+$ /ATP ratio for ATP synthesis of prokaryotic V-ATPase from *Thermus thermophilus*. *Proc. Natl. Acad. Sci. U.S.A.* 2007; 104: 20256–20261 PMID: [18077374](https://pubmed.ncbi.nlm.nih.gov/18077374/)
24. Takeda M, Suno-Ikeda C, Shimabukuro K, Yoshida M, Yokoyama K. Mechanism of inhibition of the V-type Molecular Motor by Tributyltin Chloride. *Biophys. J.* 2009; 96: 1210–1217 doi: [10.1016/j.bpj.2008.10.031](https://doi.org/10.1016/j.bpj.2008.10.031) PMID: [19186155](https://pubmed.ncbi.nlm.nih.gov/19186155/)
25. Soga N, Kinoshita K Jr., Yoshida M, Suzuki T. Kinetic equivalence of transmembrane pH and electrical potential differences in ATP synthesis. *J. Biol. Chem.* 2012; 287: 9633–9639 doi: [10.1074/jbc.M111.335356](https://doi.org/10.1074/jbc.M111.335356) PMID: [22253434](https://pubmed.ncbi.nlm.nih.gov/22253434/)
26. Parra KJ, Kane PM. Reversible association between the  $V_1$  and  $V_0$  domains of yeast vacuolar  $H^+$ -ATPase is an unconventional glucose-induced effect. *Mol. Cell Biol.* 1998; 18: 7064–7074 PMID: [9819393](https://pubmed.ncbi.nlm.nih.gov/9819393/)
27. Kane PM. Targeting Reversible Disassembly as a Mechanism of Controlling V-ATPase Activity. *Curr. Protein Pept. Sci.* 2012; 13: 117–123 PMID: [22044153](https://pubmed.ncbi.nlm.nih.gov/22044153/)
28. Tani K, Arthur CP, Tamakoshi M, Yokoyama K, Mitsuoka K, Fujiyoshi Y, et al. Visualization of two distinct states of disassembly in the bacterial V-ATPase from *Thermus thermophilus*. *Microscopy* 2013; 62: 467–474.